Light-pulse propagation in Fibonacci quasicrystals

Mher Ghulinyan,* Claudio J. Oton,† Luca Dal Negro,‡ and Lorenzo Pavesi
Department of Physics, University of Trento and INFM, via Sommarive 14, I-38050 Povo (Trento) Italy

Riccardo Sapienza, Marcello Colocci, and Diederik S. Wiersma§
European Laboratory for Nonlinear Spectroscopy, INFM, and Department of Physics, University of Florence, via Nello Carrara 1, 50019 Sesto Fiorentino (Florence), Italy

(Received 23 February 2004; revised manuscript received 23 September 2004; published 16 March 2005)

We report on an extensive study on light propagation in Fibonacci quasicrystals, with special focus on the optical states around the fundamental band gap of the structure. The samples are fabricated using free-standing porous silicon and experiments are performed using an ultrafast time-resolved transmission technique. Large pulse delays and pulse stretching are observed when exciting the band edge states of the Fibonacci structure. We carefully describe the various details concerning sample preparation and optical experiments. In particular, we highlight how optical path gradients related to technical limitations of the standard sample fabrication technique are responsible for a spatial confinement and intensity reduction of the narrow band edge states. However, band edge related pulse delay and stretching effects can still be observed experimentally in the time domain because the characteristic features originating from the quasiperiodic order are preserved. Experiments and numerical calculations are in good agreement.

DOI: 10.1103/PhysRevB.71.094204 PACS number(s): 42.25.Hz, 42.25.Dd, 42.70.Qs, 71.23.Ft

I. INTRODUCTION

Transport phenomena of light waves in three-, two-, and one-dimensional complex structures have attracted a lot of attention in the last decade.[1] Complex photonic structures are artificial materials in which the refractive index has a particular variation on length scales comparable to the wavelength of light. A periodic variation of the refractive index gives rise to a photonic crystal structure. At high enough refractive index contrast these periodic systems can exhibit a photonic band gap, in analogy with the energy band gap for electrons in a semiconductor.[2] When the periodicity of the photonic crystal structure is broken, light propagation is not described by Bloch states. The opposite extreme of a periodic system is a fully random structure in which light waves perform a random walk. To first approximation, light transport can then be described as a diffusion process. In addition, interference effects can play a crucial role in disordered structures, in close analogy to the transport of electrons in disordered systems. Examples of interesting interference phenomena in disordered optical materials are weak[3] and strong[4] localization of light, short-long range speckle correlations[5] and universal conductance fluctuations.[6] Complex dielectric systems are expected to play an important role in a wide range of photonic applications, for instance as photonic crystal filters and wave guides,[2] and in the form of amplifying random materials that can act as laser sources.[7]

These light transport phenomena are often easier to investigate in one-dimensional (1D) multilayer structures. 1D multilayers can be realized in a controlled manner[8,9] and allow for an exact theoretical description.[10] Ordered dielectric multilayer structures are widely used as highly reflective Bragg mirrors with limited bandwidth. The introduction of a defect layer turns them into a narrow-band filter with a transmission state within the forbidden band gap.

Periodic and random structures cover only the two extremes of the rich spectrum of complex dielectric structures. Quasicrystals[11] form a class of systems in the intermediate regime and have fascinating properties. In these deterministic nonperiodic structures translational order is absent. Among the various 1D quasicrystals, the Fibonacci binary quasicrystal has been the subject of an extensive theoretical and experimental effort in the last two decades. In 1985 Merlin *et al.* reported the first realization of electronic quasiperiodic Fibonacci superlattices[12] which was followed by several experimental and theoretical studies on electron transport in these systems.[13] The optical analogue of the Fibonacci structure is realized by stacking two different dielectric layers according to a simple generation rule.[14,15] The typical structure of the optical mode density (DOM) in a Fibonacci system has a self-similar nature[16] and consists of narrow resonances separated by numerous *pseudo band gaps*, where the DOM tends to zero[14,17] [see Fig. 1(a)]. The band gaps are a consequence of the multifractal nature of the Fibonacci quasiperiodic structure. Moreover, the optical modes of a Fibonacci quasicrystal are critically localized, with an intensity profile decaying less than exponentially.[18]

Recently we have reported the first experimental study on light transport through the band edge resonances of a 1D optical Fibonacci system.[19] The Fibonacci multilayer was realized in porous silicon on a silicon substrate. A pulsed interferometry technique was used to investigate the nature of the band edge states. Mode beating, sizable field enhancement, strong pulse stretching, and a strongly reduced group velocity in the band edge region around a Fibonacci pseudogap were shown.

In these initial studies our time-resolved setup allowed to investigate the band edge states of a band gap at ~2000 nm. In addition, the control over the growth parameters of thick structures resulted in a 6% negative gradient in the layer thickness and 10% positive gradient in the porosity (optical thickness decreasing with depth). Numerical studies of the DOM show that the fundamental Fibonacci band gap (FBG)

 ©2005 The American Physical Society

is more robust against the optical path gradients than other band gaps [Fig. 1]. Following our recent improvements in porous silicon multilayers growth[8] and time-resolved techniques,[20] in the present study we managed to grow highly homogeneous Fibonacci structures and to study the light transport at the fundamental band gap (FBG).

In this paper we present several experimental and sample preparation details, using a simplified time-resolved technique to study the time response of these systems. We use free-standing samples where the Fibonacci system was detached from the silicon substrate. The availability of free-standing samples allows to grow thick structures with high optical quality, limiting the total drifts to about 4%. This value leads to a mode structure [Fig. 1(b)] which, at the FBG, is very similar to the ideal case. On these samples we perform time-resolved transmission experiments using a simplified technique. We compare the effects observed in Ref. 19 at a higher order pseudogap to the behavior of the fundamental band gap. Also we investigate the delicate interplay between quasiperiodicity and optical path gradients due to natural growth drifts. We find that growth drifts can still lead to the observation of strong pulse delay in the band edge region even though the narrow transmission peaks of a sample with optical path drift are barely distinguishable in a usual transmission spectrum. We show that the optical path gradient tilts the photonic band structure and spatially confines the band edge states, without affecting their specific nature reflecting the Fibonacci quasiperiodicity. The measured transmitted signals are analyzed and numerical calculations of time-resolved transmission and pulse delay times are carried out using a transfer-matrix method. The calculations show good agreement with the experimental results.

The paper is organized as follows. In Sec. II we describe the sample preparation technique and optical characterization of the samples by transmission measurements, together with the transfer-matrix calculations of the spectrum and definition of the optical parameters of the structures. We describe also the details of the ultrafast time-resolved transmission measurements. In Sec. III we discuss the results of the time-resolved measurements in the band edge region of the 12th order Fibonacci sample. A detailed discussion of the drift-induced effects, like the band gap tilting, and the differences between the transmission spectra and DOM is given. An analysis of the delay time dependence on optical thickness drift is presented as well. Finally, Sec. IV gives the summary of our results and the conclusions.

II. EXPERIMENT

A. Sample preparation

A Fibonacci sequence of order j can be constructed from two building blocks, say A and B, following the Fibonacci generation rule $S_{j+1}=\{S_{j-1}S_j\}$ for $j \geqslant 1$; with $S_0=\{B\}$ and $S_1=\{A\}$. The lower order Fibonacci sequences are therefore $S_2=\{BA\}$, $S_3=\{ABA\}$, $S_4=\{BAABA\}$, etc. For a 1D dielectric Fibonacci sample, the elements A and B are dielectric layers with different refractive indices and thickness.

The choice for the starting layer refractive index is arbitrary, and one can build the structure choosing layer A to have high (low) and layer B low (high) refractive indices. The structures obtained in this way do not necessarily have the same optical properties but are strongly related. The numerical calculations of the so-called scattering states maps[19] of the 12th order Fibonacci structure, for the two cases $n_A < n_B$ and $n_A > n_B$ show that the light distribution inside the structures is very similar. In the experiment described here we chose the layer A to be of the high refractive index type. The physical thickness of the layers was chosen such that the optical thickness of both layers was equal to $\lambda_0/4$, where λ_0 is the central wavelength of the spectrum. This choice satisfies the maximum quasiperiodicity condition.[14]

We realized the dielectric Fibonacci samples by electrochemical etching of silicon. Porous silicon has interesting optical properties[21] and, if grown in highly doped p-type silicon, behaves as an optically homogeneous dielectric material with an effective refractive index n determined by its porosity. As porous silicon is fabricated by a self-limiting electrochemical process, one can control the refractive index of each layer by varying the electrochemical current during the fabrication.[21] The thickness of the porous layers is determined by the etching duration.

Fibonacci samples were etched by starting from (100)-oriented p^+-type silicon (resistivity 0.01 Ω cm). The electrolyte was prepared mixing a 30% volumetric fraction of aqueous HF (48 wt. %) with ethanol. A magnetic stirrer was used to improve electrolyte exchange. The applied current density defined the porosity of the layer. We applied 7 mA/cm^2 for the low porosity layer A (refractive index $n_A=2.13$) and 50 mA/cm^2 for the high porosity layer B ($n_B=1.45$). These current values are limited by the requirement to maintain high optical quality all over the 233 layers. The low current value is chosen such that sufficient electrolyte exchange remains through the small pores, while the high current value is limited by the requirement of mechanically stable layers. Alternating these two currents we created the multilayer and, finally, a high current pulse of 400 mA/cm^2 was applied for 1 second to detach the multilayer structure from the substrate. This way, free-standing Fibonacci samples of the ninth (55 layers) and 12th order (233 layers) were grown, centered in the near infrared wavelength region (NIR).

The etching process introduces a natural drift in the layer porosity and thereby in the optical thickness of the layers. By comparing the reflection spectra taken from both sides of the Fibonacci superlattice we can define accurately the natural drift values.[8] Once the natural drift is evaluated, new samples can be grown with efficient compensation by correcting the duration of the etching process for each layer (see Ref. 8 for details). This is especially relevant in realizing thick structures and limits the porosity drift to 4% for the samples with 233 layers. Without compensation the natural drift in these thick samples is about 6% in the layer thickness and 10% in the layer porosity.[19] For the ninth order Fibonacci sample the compensation procedure limits the drift to 1%. A 5% drift value was reported in Ref. 14 for a ninth order Fibonacci quasicrystal grown by electron-gun evaporation.

Transmission and reflectance spectra of the free-standing samples were measured from 800 to 2500 nm with a Varian Cary-5000 UV-VIS-NIR spectrophotometer with halogen lamp and a collimated beam with 1 mm spot diameter. The

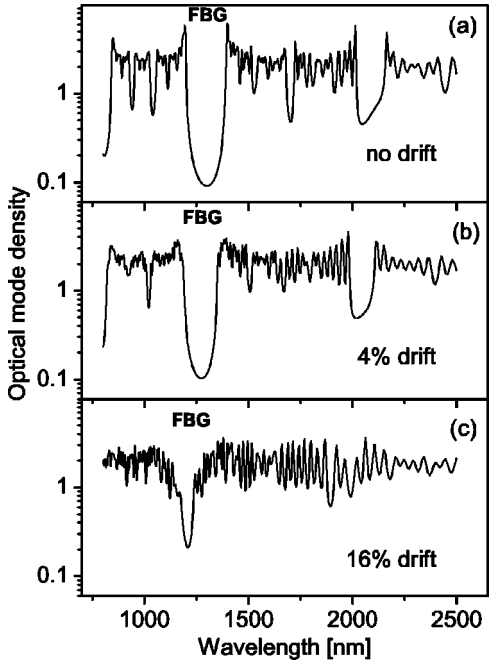

FIG. 1. The calculated density of optical modes of a 12th order 1D Fibonacci quasicrystal for various degrees of optical path drifts: (a) ideal structure with no drift, (b) 4% drift, (c) 16% drift. The blueshift of the spectral features with increasing the drift is due to the reduced optical thickness of the layers. FBG refers to the fundamental band gap.

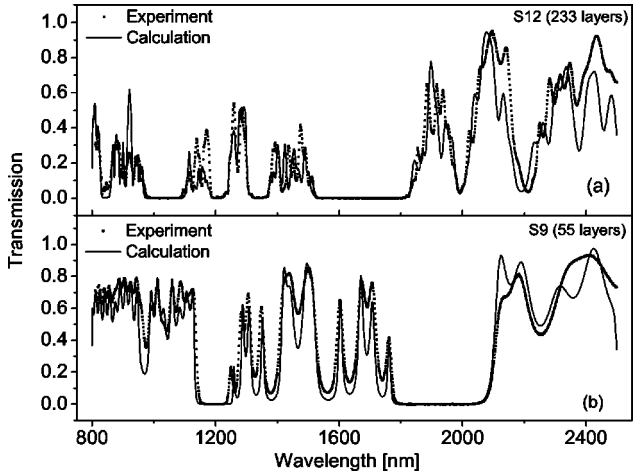

FIG. 2. Transmission spectra of Fibonacci samples S_9 (a) and S_{12} (b). The solid lines are the results of a transfer-matrix calculation assuming optical path drifts of 1% (for S_9) and 4% (for S_{12}) and optical losses (mainly scattering by the mesopores) of $\alpha \sim 120\ \mathrm{cm}^{-1}$. The dots denote the measured spectra.

overall wavelength resolution of the system was 2 nm. The transmission spectra of ninth and 12th order Fibonacci samples are reported in Fig. 2. The band gaps manifest as low transmission regions (stop-bands) in the transmission spectra. A more detailed analysis of the presence of the pseudogap can be performed by looking at the DOM of these structures,[22] as we will discuss later. Band gaps are clearly visible for both samples.

In order to interpret the transmission spectra and to check the parameters of the multilayers, we have calculated numerically their transmission spectra using a transfer-matrix approach.[9] In the calculations, the dispersion of the optical constants has been taken into account. The calculations for the S_9 and S_{12} samples, assuming, respectively, a 1% and 4% drift and total loss coefficient α of $\sim 120\ \mathrm{cm}^{-1}$ (mainly determined by scattering losses), are reported in Fig. 2. It is known that porous silicon samples suffer from lateral inhomogeneities due to doping variations of the silicon wafers,[8] which leads to a widening of the peaks in the transmission spectra. Therefore a 1% spectral spread due to lateral inhomogeneities has been taken into account in the calculation. A good agreement is observed for both Fibonacci samples over a wide spectral range.

B. Time-resolved transmission measurements

The time-resolved data reported in this paper were obtained by ultrafast time-resolved transmission measurements using a standard optical gating technique (based on upconversion). This apparatus has the advantage of being simpler compared to a more delicate interferometric system, but it is only sensitive to the transmitted intensity and not the phase. The setup is sketched in Fig. 3. Ultrashort pulses with central wavelength $\lambda_1 = 810$ nm (pulse duration 130 fs, average power 2.0 W, repetition rate 82 MHz) were obtained with a Ti:sapphire mode-locked laser. These were used to excite an optical parametric oscillator (OPO) system (Spectra-physics OPAL), from which tunable pulses (at wavelength λ_2 between 1400 and 1570 nm) with 220 fs pulse duration were obtained (bandwidth about 14 nm, average power 100 mW).

The pulses were focused on a small spot on the sample ($\sim 30\ \mu$m diameter). The transmitted signal was mixed in a nonlinear BBO (beta barium borate) crystal, together with a

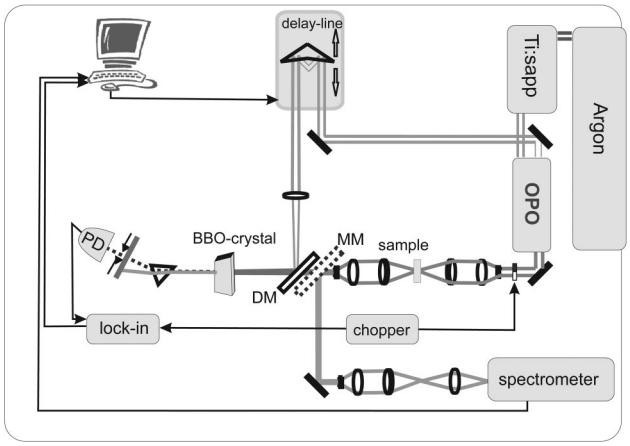

FIG. 3. Time-resolved transmission setup based on an optical gating technique. When the movable mirror (MM) is in position, the spectral response of the sample is monitored through a spectrometer. If the mirror MM is removed, then the infrared beam is mixed, after the dichroic mirror (DM), with the residual Ti:sapphire beam in the nonlinear BBO crystal. The upconverted signal is monitored via a photodiode (PD) and a lock-in technique is used to reduce noise.

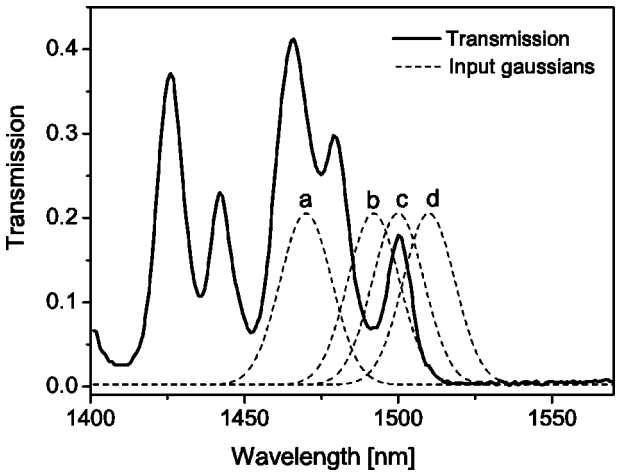

FIG. 4. Measured transmission spectrum of the sample S_{12} in the region in which the OPO can be tuned (solid line). The Gaussian curves (dashed lines) represent the spectra of some input pulses [named (a), (b), (c), and (d)].

reference pulse (450 mW), the latter being obtained from the residual Ti:sapphire beam and delayed in time via a controlled delay line. The sum frequency signal was selected with a prism and detected with a photodiode. A standard lock-in technique was used to suppress noise. Background light was suppressed with narrow band filters and spatial filtering. Since the sum frequency is proportional to the temporal overlap between signal and reference pulse, the time

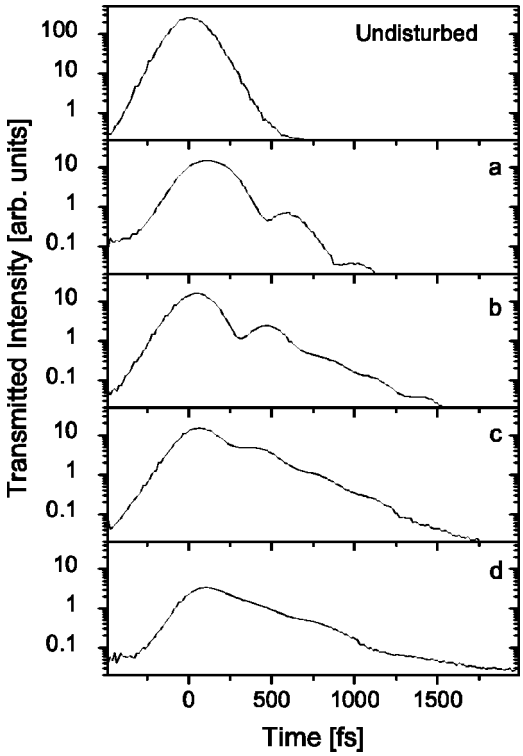

FIG. 5. Time-resolved transmitted signal through the S_{12} sample. The undisturbed pulse is shown in the top plot, and plots (a), (b), (c), and (d) are the transmitted pulses at wavelengths 1470, 1492, 1500, and 1510 nm, respectively.

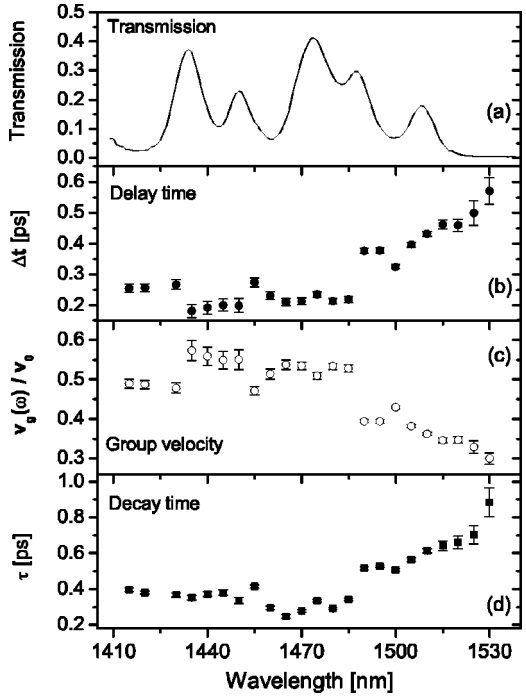

FIG. 6. (a) Measured transmission spectrum of S_{12}. (b) Delay time of the center of mass of the transmitted pulse amplitude with respect to the undisturbed one. (c) Group velocity (as derived from the delay time) with respect to the group velocity in a medium with an effective refractive index equal to the weighted average of the refractive indices of the constituent layers. (d) Decay time of the transmitted signal.

profile of the transmitted signal can be mapped by varying the delay of the reference. The overall temporal resolution of our system was measured to be around 260 fs.

III. RESULTS AND DISCUSSION

A. Analysis of the measured data

We performed time-resolved transmission measurements on the band edge regions of the 12th order Fibonacci samples (S_{12}). While in Ref. 19 we have investigated the long wavelength edge of a higher order band gap, here we report measurements in the wavelength region of the short wavelength edge of the fundamental band gap, for comparison. No time-resolved measurements were possible on the ninth order sample due to the limited time resolution of our system.

Figure 4 shows the detailed transmission spectrum of the S_{12} sample together with four typical [(a)–(d)] spectra of the incoming laser pulses (dotted lines) in the range where the time-resolved measurements were performed. We have probed the structure at different wavelengths around the band edge region in order to excite the band edge states. The time-resolved transmission of these four pulses [(a)–(d)] is shown in Fig. 5. The undisturbed pulse (with no sample) is also reported in the plot.

The zero of the time axis in Fig. 5 is the time at which the maximum of the unperturbed pulse arrives on the detector.

We have corrected for the trivial delay of the pulse due to the additional optical path of the sample. That is, the sample of 44 μm thickness has an optical thickness of 76 μm. An average effective refractive index $n_{\text{eff}} \approx 1.88$ has been calculated by the formula $n_{\text{eff}} = \Sigma(n_i d_i)/\Sigma d_i$, where d_i is the physical thickness of the ith layer in the structure. The time offset due to this effect is 99 fs for all pulses that pass through a 12th order Fibonacci sample. We have corrected for this so that the pulse delays, visible for curves [(a)–(d)] in Fig. 5, are purely due to the internal optical mode structure (internal resonances) inside the sample. Note that by using free-standing porous silicon Fibonacci structures one avoids large time-offsets due to the silicon substrate.

As the wavelength of the signal is increased, i.e., as we approach the band gap, the shape of the transmitted pulses changes. In particular, the pulses are delayed and stretched. In addition, when two states are excited simultaneously, mode beating occurs at a beating frequency given by the frequency separation of the states. In Fig. 6 we have plotted the delay of the center of mass of the pulses and the decay time for several measurements in the wavelength range between 1410 and 1530 nm, i.e., the short wavelength edge of the fundamental band gap. As in Ref. 19, the delay time was calculated from the delay of the center of mass of the transmitted electric field envelope of the signal pulse [Fig. 6(b)]. Since the detection method employed in this paper provides directly the signal intensity, the square root of the measured intensity profiles was taken to determine the center of mass of the amplitudes. From the delay time, the group velocity v_g of the wave packet with respect to the light velocity v_0 in a medium with effective refractive index of $n_{\text{eff}} \approx 1.88$ is deduced and reported in Fig. 6(c). A maximum group velocity reduction of $v_g/v_0 \approx 0.29$ is found at the band edge frequencies. The electric field of the transmitted pulses decays almost exponentially with time. The obtained decay time constants extracted from the raw data are shown in Fig. 6(d).

Both the delay and the decay times increase as we approach the band gap. One expects that these should be accompanied by narrow peaks in the transmission spectrum at the edge of the band gap, corresponding to high peaks in the DOM. The reason for not observing narrow peaks in transmission (Fig. 4) is the technical limitation of the method used to obtain the transmission spectra. The transmission spectra were recorded by using a broad source with a large spot of $\sim$1 mm in diameter on the sample surface and a limited spectral resolution.

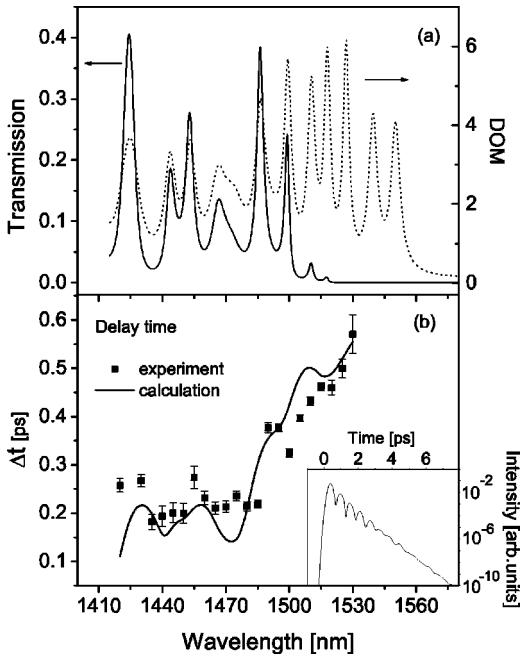

FIG. 7. (a) Calculation of the transmission spectrum (solid line) of the S_{12} sample and (dashed) corresponding density of modes (DOM). (b) Measured delay times of the transmitted pulse (filled squares) and the transfer-matrix calculation (solid line). The inset shows an example of a calculated time-resolved transmitted intensity for a probe pulse centered at 1497 nm.

B. Numerical calculation of light propagation through the Fibonacci sample

We have calculated the optical response of the S_{12} sample using a transfer matrix approach. The time-response of the system was obtained by inverse fast Fourier transformation (inverse FFT) of the product of the spectrum of the incoming pulse and the transmission spectrum,

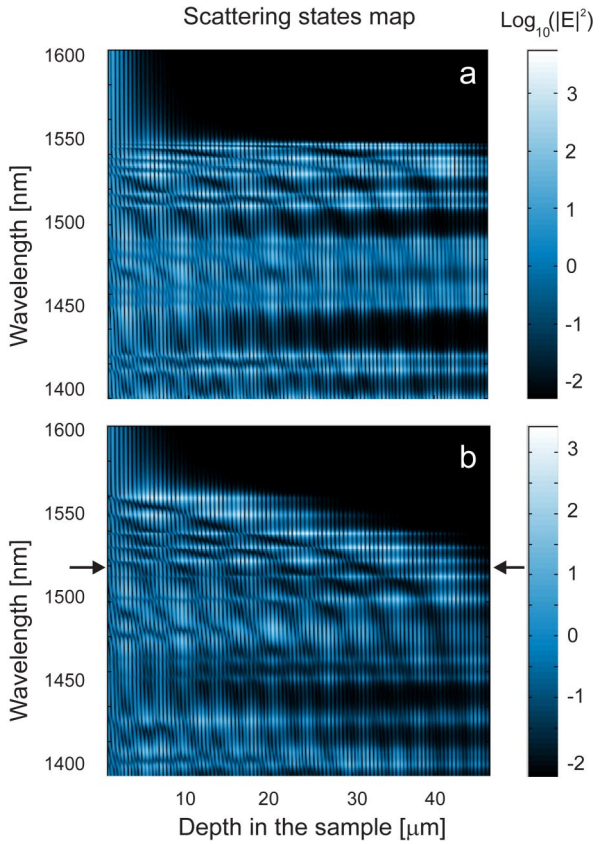

FIG. 8. (Color online) Scattering states map of the S_{12} sample: (a) ideal structure, (b) 4% drift. The arrows in the lower graph indicate the wavelength above which the transmission becomes nearly zero, while internal resonances can be clearly identified.

$$T(t) = \mathcal{F}^{-1}[G(\omega)T(\omega)] = \int_{-\infty}^{\infty} G(\omega)T(\omega)\exp(i\omega t)d\omega, \quad (1)$$

where $T(t)$ is the transmitted time-resolved signal, $G(\omega)$ is the (Gaussian) spectral profile of the incoming pulse, and $T(\omega)$ is the transmission spectrum of the Fibonacci sample.

The temporal profiles of the transmitted pulses were calculated for various wavelengths, and the corresponding delay times were extracted. Figure 7(a) shows the calculated transmission spectrum (solid line) and the density of modes (dashed line) of the S_{12} sample in the wavelength region where the time-resolved measurements were performed. The transmission appears to vanish above a wavelength of about 1520 nm, while the DOM shows peaks until 1550 nm. A comparison between transmission spectra, DOM, and group velocity of a periodic, an ideal Fibonacci, and a Fibonacci structure with drift is reported in Ref. 23. In an ideal structure without drifts, both the transmission and DOM vanish in the band gap region. When the drift is present, the low transmission regime extends for a wider wavelength range than the DOM gap.

The reason can be found by looking at the calculated scattering states map of the Fibonacci sample, reported in Fig. 8. The scattering states map for the ideal case with flat photonic band structure is shown in Fig. 8(a). The drift in the optical thickness acts as a built-in bias that tilts the band edge [see Fig. 8(b)]. The tilting behaves as the analogue of an external electric field applied to an electronic superlattice structure. We exploited recently this analogy to observe time-resolved photonic Bloch oscillations in optical superlattice structures.[20]. In the 12th order Fibonacci sample, the tilt reduces the spatial extension of the optical modes close to the band gap. The first band edge states, therefore, do not extend over the whole sample and their contribution to the transmission spectrum is strongly reduced. As a result, the transmission spectra and density of modes differ in the region of the band gap. Note that the transmission for wavelengths above 1520 nm is not truly zero but simply too small to be visible in a linear scale plot. The long delay times observed around the edge of the band gap can be associated with the time needed to propagate through the band edge states. The long decay times are directly related to the spatial confinement of these states leading to a resonance with high Q-factor. In Fig. 7(b) a comparison between the calculated and the measured delay times is reported. The correspondence between the experiment and calculation is very good. An example of the calculation of the transmitted pulse is shown in the inset of Fig. 7(b) for a probe pulse centered at a wavelength of 1497 nm. One can see the oscillating behavior of the transmitted signal due to the beating between the sharply defined modes at 1495 and 1500 nm.

C. Effect of optical path gradients

We have performed further numerical calculations to investigate the influence of drifts on light propagation through the Fibonacci sample. In Fig. 9 we show the transmission spectra [(a)–(c)], DOM [(d)–(f)], and the calculated pulse delays [(g)–(i)] for 12th order Fibonacci samples for different values of the optical thickness drift. In an ideal (no drift) S_{12} structure the DOM exhibits a band gap above $\lambda = 1540$ nm [Fig. 9(d)]. Sharp, critically localized optical states are observed at the band edge, that correspond to peaks in the transmission spectrum [Fig. 9(a)]. Consequently, the transmission spectrum shows no transmission for wavelengths in the band gap. The maximum values of the pulse delay time are found in the band edge region [Fig. 9(g)]. The pulse delays are due to the band edge dispersion of an ideal Fibonacci superlattice.

When a linear drift of 4% is introduced in the optical thickness of the sample (the optical thickness changes linearly with depth and the optical path difference between the

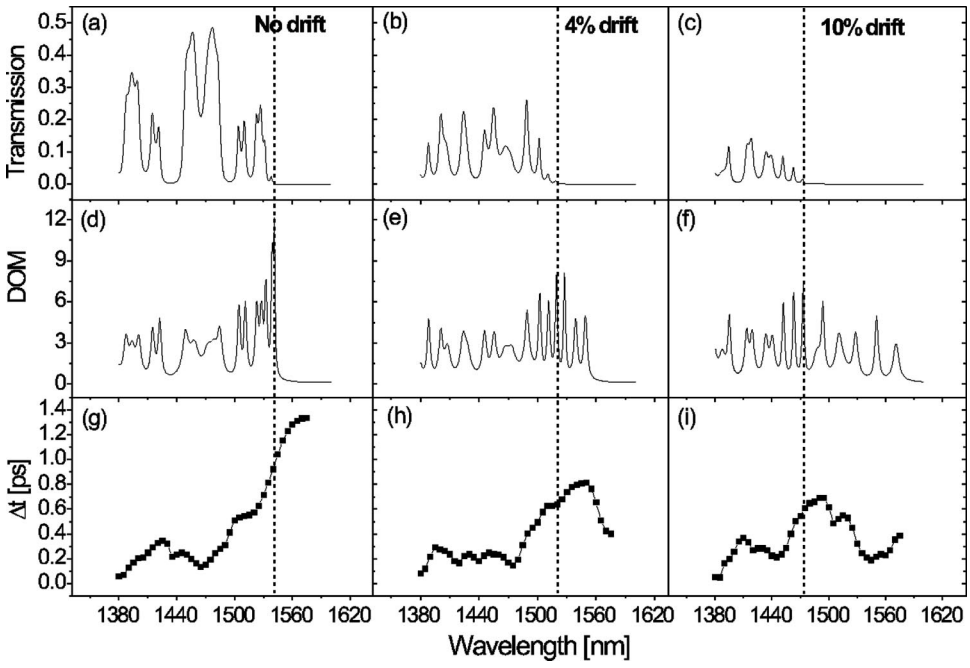

FIG. 9. Transfer matrix calculations of the transmission spectra [(a)–(c)], the corresponding density of modes [(d)–(f)], and the pulse delay times [(g)–(i)] of the S_{12} structure with the loss value of 120 cm^{-1} and different values of drift: (a) 0%, (b) 4%, and (c) 10% are shown. The dashed lines are a guide to the eye that mark the borders between the high and negligible transmission regions.

first and last layer is 4%), optical states appear in the wavelength region where previously the band gap was present [Fig. 9(e)]. The band edge shifts thereby to higher wavelengths and the band gap consequently narrows. (See also Fig. 1.) The first few band edge states are now hardly visible in the transmission spectrum. Due to the tilted band edge the transmission coefficient of these modes is reduced. In addition also the associated time delay is somewhat reduced, as can be seen in Fig. 9(h). Note that the wavelength dependence of the delay time starts to differ from that of the ideal structure where the transmission becomes negligible. All these trends are more pronounced when the drift in the optical thickness is increased to 10%, as reported in Figs. 9(c), 9(f), and 9(i).

In Fig. 10 we report the intensity distribution inside the sample of the first four optical modes at the band edge for the case of an ideal Fibonacci structure and the case of 4% drift. The top panels show the DOM around the band edge. In absence of drift, the intensity distribution shows the characteristic self-similar structure of the band edge resonances of a Fibonacci quasicrystal.[24] When the drift is introduced (right panels), the main features remain the same but the distribution becomes asymmetric with its center of mass towards the front side of the sample. Due to the drift, the mode is confined between the sample surface and the tilted band gap. This is the behavior of a Fibonacci quasicrystal with built-in bias. The calculations show that the natural drift occurring during the growth of the Fibonacci samples does affect the spatial extension of the first few band edge modes, but it does not destroy their specific structure. The higher order band edge modes are hardly affected by the natural drift.

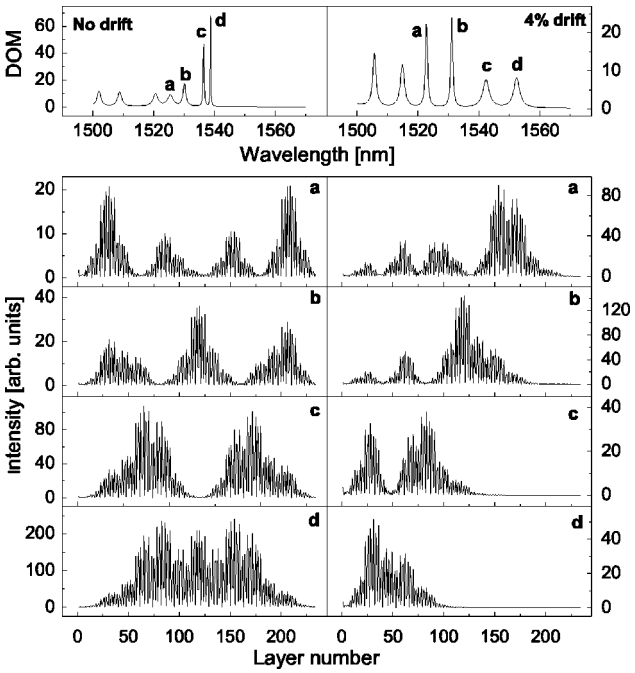

FIG. 10. Intensity distribution inside the sample of the first four band edge states in an ideal Fibonacci structure (left) and a 4% drifted one (right). The density of modes (DOM) around the Fibonacci band edge is shown in the upper panels for both cases.

IV. CONCLUSIONS

In this work we have investigated the propagation of optical pulses through Fibonacci quasicrystals, with a special focus on the wavelength regime around the band edge. We performed time-resolved measurements around the fundamental band gap using an ultrafast time-resolved transmission technique. The transmitted signals showed large delays and strong pulse stretching close to the band gap. A strongly reduced group velocity, associated with large delay times, was observed and verified through calculations. In addition, we showed that the optical path gradient acts as a built-in bias which tilts the photonic band structure. Delayed and stretched pulses can still be detected, however, even with optical drift.

ACKNOWLEDGMENTS

The authors wish to thank Zhao Qing Zhang, Zeno Gaburro, Daniel Navarro, Maurizio Artoni, Costas Soukoulis, and Roberto Righini for interesting discussions. This work was financially supported by the INFM projects RANDS and Photonic and by MIUR through the Cofin 2002 "Silicon based photonic crystals" and FIRB "Sistemi Miniaturizzati per Elettronica e Fotonica" and "Nanostrutture molecolari ibride organiche-inorganiche per fotonica" projects.

*www.science.unitn.it/~semicon; mghool@science.unitn.it

†Present address: Departamento de Fisica Basica, University of La Laguna, Avda. Astrofísico Fco. Sánchez s/n, La Laguna 38204 Tenerife, Spain.

‡Present address: Materials Processing Center, Department of Materials Science and Engineering, Massachusetts Institute of Technology, Building 13, Room 41-34, 77 Massachusetts Avenue, Cambridge, MA 02139.

§www.complexphotonics.org; wiersma@lens.unifi.it

[1] See, e.g., Ping Sheng, *Introduction to Wave Scattering, Localization, and Mesoscopic Phenomena* (Academic, New York, 1995); *Wave Scattering in Complex Media: From Theory to Applications*, edited by B. A. van Tiggelen and S. E. Skipetrov, Nato Science Series II: Mathematics, Physics and Chemistry 107 (Kluwer, Dordrecht, 2002).

[2] See, e.g., E. Yablonovitch, Phys. Rev. Lett. **58**, 2059 (1987); S. John, *ibid.* **58**, 2486 (1987); *Photonic Band Gap Materials*, edited by C. M. Soukoulis (Kluwer, Dordrecht, 1996); J. D. Joannopoulos, R. D. Meade, and J. N. Winn, *Photonic Crystals: Molding the Flow of Light* (Princeton University Press, Princeton, NJ, 1995).

[3] Y. Kuga and A. Ishimaru, J. Opt. Soc. Am. A **8**, 831 (1984); M.

P. van Albada and A. Lagendijk, Phys. Rev. Lett. **55**, 2692 (1985); P. E. Wolf and G. Maret, *ibid.* **55**, 2696 (1985).

[4] P. W. Anderson, B. I. Halperin, and C. M. Varma, Philos. Mag. **25**, 1 (1972); S. John, Phys. Rev. Lett. **53**, 2169 (1984); R. Dalichaouch, J. P. Armstrong, S. Schultz, P. M. Platzman, and S. L. McCall, Nature (London) **354**, 53 (1991); A. Z. Genack and N. Garcia, Phys. Rev. Lett. **66**, 2064 (1991); D. S. Wiersma, P. Bartolini, A. Lagendijk, and R. Righini, Nature (London) **390**, 671 (1997).

[5] N. Garcia and A. Z. Genack, Phys. Rev. Lett. **63**, 1678 (1989); M. P. van Albada, J. F. de Boer, and A. Lagendijk, *ibid.* **64**, 2787 (1990).

[6] F. Scheffold and G. Maret, Phys. Rev. Lett. **81**, 5800 (1998).

[7] D. Wiersma, Nature (London) **406**, 132 (2000); S. Mujumdar, M. Ricci, R. Torre, and D. S. Wiersma, Phys. Rev. Lett. **93**, 053903 (2004).

[8] M. Ghulinyan, C. J. Oton, G. Bonetti, Z. Gaburro, and L. Pavesi, J. Appl. Phys. **93**, 9724 (2003); M. Ghulinyan, C. J. Oton, Z. Gaburro, P. Bettotti, and L. Pavesi, Appl. Phys. Lett. **82**, 1550 (2003).

[9] L. Dal Negro, M. Stolfi, Y. Yi, J. Michel, X. Duan, L. C. Kimerling, J. LeBlanc, and J. Haavisto, Appl. Phys. Lett. **84**, 5186 (2004).

[10] J. B. Pendry, Adv. Phys. **43**, 461 (1994); A. Kavokin, G. Malpuech, A. Di Carlo, P. Lugli, and F. Rossi, Phys. Rev. B **61**, 4413 (2000).

[11] D. Levine and P. J. Steinhardt, Phys. Rev. Lett. **53**, 2477 (1984); T. Fujiwara and T. Ogawa, *Quasicrystals* (Springer-Verlag, Berlin, 1990).

[12] R. Merlin, K. Bajema, R. Clarke, F. Y. Juang, and P. K. Bhattacharya, Phys. Rev. Lett. **55**, 1768 (1985).

[13] J. B. Sokoloff, Phys. Rev. Lett. **58**, 2267 (1987); Ch. Wang and R. A. Barrio, *ibid.* **61**, 191 (1988); E. Maciá and F. Domínguez-Adame, *ibid.* **76**, 2957 (1996); F. Steinbach, A. Ossipov, T. Kottos, and T. Geisel, *ibid.* **85**, 4426 (2000).

[14] W. Gellermann, M. Kohmoto, B. Sutherland, and P. C. Taylor, Phys. Rev. Lett. **72**, 633 (1994).

[15] T. Hattori, N. Tsurumachi, S. Kawato, and H. Nakatsuka, Phys. Rev. B **50**, 4220 (1994).

[16] J. M. Bendickson, J. P. Dowling, and M. Scalora, Phys. Rev. E **53**, 4107 (1996).

[17] See, e.g., F. Nori and J. P. Rodriguez, Phys. Rev. B **34**, 2207 (1986); R. B. Capaz, B. Koiller, and S. L. A. de Queiroz, *ibid.* **42**, 6402 (1990).

[18] C. M. Soukoulis and E. N. Economou, Phys. Rev. Lett. **48**, 1043 (1982); M. Kohmoto, B. Sutherland, and K. Iguchi, *ibid.* **58**, 2436 (1987); T. Fujiwara, M. Kohmoto, and T. Tokihiro, Phys. Rev. B **40**, 7413 (1989).

[19] L. Dal Negro, C. J. Oton, Z. Gaburro, L. Pavesi, P. Johnson, A. Lagendijk, R. Righini, M. Colocci, and D. S. Wiersma, Phys. Rev. Lett. **90**, 055501 (2003).

[20] R. Sapienza, P. Costantino, D. Wiersma, M. Ghulinyan, C. Oton, and L. Pavesi, Phys. Rev. Lett. **91**, 263902 (2003).

[21] L. Canham, Properties of Porous Silicon, INSPEC, 1997.

[22] T. Kondo, M. Hangyo, S. Yamaguchi, S. Yano, and Y. Segawa, K. Ohtaka, Phys. Rev. B **66**, 033111 (2002).

[23] C. J. Oton, L. Dal Negro, Z. Gaburro, L. Pavesi, P. J. Johnson, A. Lagendijk, and D. S. Wiersma, Phys. Status Solidi A **197**, 298 (2003).

[24] D. S. Wiersma, R. Sapienza, S. Mujumdar, M. Colocci, M. Ghulinyan, and L. Pavesi, J. Opt. A, Pure Appl. Opt. **7**, S190 (2005).